ADP-Ribosylation

International Edition: DOI: 10.1002/anie.201600464
German Edition: DOI: 10.1002/ange.201600464

# Bioorthogonally Functionalized NAD$^+$ Analogues for In-Cell Visualization of Poly(ADP-Ribose) Formation

*Sarah Wallrodt, Annette Buntz, Yan Wang, Andreas Zumbusch, and Andreas Marx**

***Abstract:*** *Poly(ADP-ribos)ylation (PARylation) is a major posttranslational modification and signaling event in most eukaryotes. Fundamental processes like DNA repair and transcription are coordinated by this transient polymer and its binding to proteins. ADP-ribosyltransferases (ARTs) build complex ADP-ribose chains from NAD$^+$ onto various acceptor proteins. Molecular studies of PARylation thus remain challenging. Herein, we present the development of bioorthogonally functionalized NAD$^+$ analogues for the imaging of PARylation in vitro and in cells. Our results show that 2-modified NAD$^+$ analogues perform remarkably well and can be applied to the in-cell visualization of PARylation simultaneously in two colors. This tool gives insight into the substrate scope of ARTs and will help to further elucidate the biological role of PARylation by offering fast optical, multi-channel read-outs.*

Having celebrated its 50th anniversary in 2013,[1] research on poly(ADP-ribose) (PAR; Figure 1) has recently experienced a renaissance owing to discoveries of the importance of PAR as a posttranslational protein modification and signaling molecule.[2] This biopolymer is involved in fundamental processes such as the DNA damage response[3] and gene regulation,[4] as well as in cellular physiology[5] and apoptosis.[6] It is thus not surprising that various pathophysiological conditions and disease states, most prominently in cancers, are associated with altered PARylation.[5b,7]

ADP-ribosylation is catalyzed by ADP-ribosyltransferases (ARTs). In humans, 17 family members have been identified, with ADP-ribosyltransferase diphtheria toxin like 1 (ARTD1) being the best studied.[8] In a typical reaction, ADP-ribose from nicotinamide adenine dinucleotide (NAD$^+$) is covalently transferred onto distinct side chains of substrates to give mono(ADP-ribos)ylation. Multiple additions of up to 200 ADP-ribose units onto the 2′-OH results in poly(ADP-ribos)ylation. Branching occurs through elongation at the 2″-OH with an average frequency of one per 20 to 50 units of linear polymer (see Figure 1).[2] Besides its many substrates, ARTD1 serves as its own acceptor[9] in a process called auto(ADP-ribos)ylation.

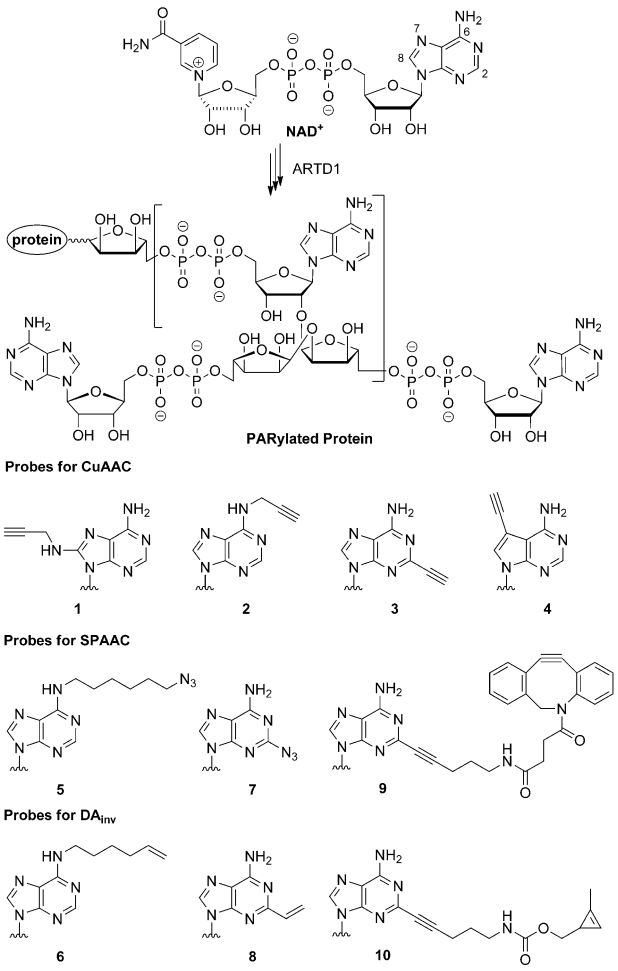


***Figure 1.*** Structures of poly(ADP-ribose), NAD$^+$, and NAD$^+$ analogues **1**–**10**.

Owing to its broad functions, it is of utmost importance to study PARylation on a cellular level. However, only very few tools are available to date that enable the direct cellular imaging of PAR.[10] Indirect methods used for visualization include PAR-specific antibodies[11] and ADP-ribose-binding macrodomains.[12] Recently, "clickable" alkyne-tagged NADs[13] have been applied for research on PARylation processes. However, imaging applications in cellular systems have not yet been described.

Herein, we report the development of functionalized NAD$^+$ analogues (Figure 1) for the intracellular imaging of PAR based on bioorthogonal chemistry. In order to explore the best substrate properties, we systematically varied the positions as well as the types of modification, thereby allowing both copper(I)-mediated and copper-free click

[*] S. Wallrodt, A. Buntz, Dr. Y. Wang, Prof. Dr. A. Zumbusch, Prof. Dr. A. Marx
Department of Chemistry, University of Konstanz
Universitätsstraße 10, 78457 Konstanz (Germany)
E-mail: andreas.marx@uni-konstanz.de
Homepage: http://www.uni-konstanz.de/chemie/~agmarx

Supporting information for this article can be found under: http://dx.doi.org/10.1002/anie.201600464.

  

reactions. The compounds described herein are equipped with 1) an alkyne for copper(I)-catalyzed azide–alkyne cycloaddition (CuAAC);[14] 2) an azide or cyclooctyne for strain-promoted azide–alkyne cycloaddition (SPAAC);[15] and 3) an alkene[16] or cyclopropene[17] for inverse electron demand Diels–Alder reactions ($DA_{inv}$). By investigating which of these new compounds are well-accepted, it was possible to gain insight into the substrate scope of ARTD1. Moreover, we applied these analogues in cellular systems and identified reporter groups that enable the selective visualization of PARylation in the cell nucleus.

First, we considered different modification sites at $NAD^+$. To circumvent interference with polymerization, we attached labels onto the purine base. Jiang et al.[13a] prepared $NAD^+$ analogues modified with alkynes in position 8 (**1**) and 6 (**2**) and showed that only **2** was used by ARTD1 to form modified polymers. Additionally, we synthesized 2-modified $NAD^+$ **3** and demonstrated its incorporation into PAR.[13b] In order to explore position 7, we synthesized the corresponding analogue **4**. For this, 7-ethynyl-7-deaza-adenosine[18] was prepared, phosphorylated, and coupled with β-nicotinamide mononucleotide to yield **4** (Scheme S1 in the Supporting Information).

All of the analogues described herein were tested in in vitro assays with ARTD1 and histone H1.2 as acceptors for ADP-ribosylation as previously reported.[13b] In brief, after incubating the respective analogue with ARTD1, short dsDNA, and H1.2, conjugation with fluorophores was performed. Following analysis by SDS PAGE, fluorescence was detected and compared to the gel with Coomassie Blue staining (Figure 2 A). Successful PARylation is indicated by 1) characteristic polymer-modified H1.2, and 2) disappearance of the ARTD1 band at 113 kDa owing to automodification. Control reactions were performed without enzyme or with natural substrates.

Compounds **3** and **4** were investigated in this assay (see Figure S1 in the Supporting Information) and then labeled by CuAAC. As before,[13b] 2-alkyne-$NAD^+$ **3** was well incorporated, whereas 7-alkyne-$NAD^+$ **4** showed no PAR formation. Placing these findings in context,[13a] we conclude that other functional groups can be introduced at positions 2 and 6 without significantly impairing ARTD1 activity.

Next, we targeted other bioorthogonal reporters and synthesized the analogous azides **5** and **7**, as well as the terminal alkenes **6** and **8**, to label PAR through either SPAAC or $DA_{inv}$ chemistry (Figure 1). The modified nucleosides were prepared,[19] phosphorylated, and converted into $NAD^+$ analogues **5**–**8** (see Scheme 1).

To our surprise, we found that ARTD1 was not able to process the 6-modified analogues **5** and **6** (Figure S2, Lane 4). However, when using a 1:1 mixture with natural $NAD^+$, incorporation was indicated by the of formation fluorescent polymers (Figure S2, Lane 5). Considering that ARTD1 is able to metabolize **2**, we conclude that the higher steric demand of these analogues hampers their substrate properties, especially for the first ADP-ribose attachment. In contrast, the 2-modified NADs **7** and **8** were well incorporated into PAR, even in absence of natural $NAD^+$, as indicated by fluorescent product (Figure S2, Lane 7). However, slow and unspecific labeling of 2-vinyl-modified PAR with tetrazines rendered this reaction unsuitable for imaging.

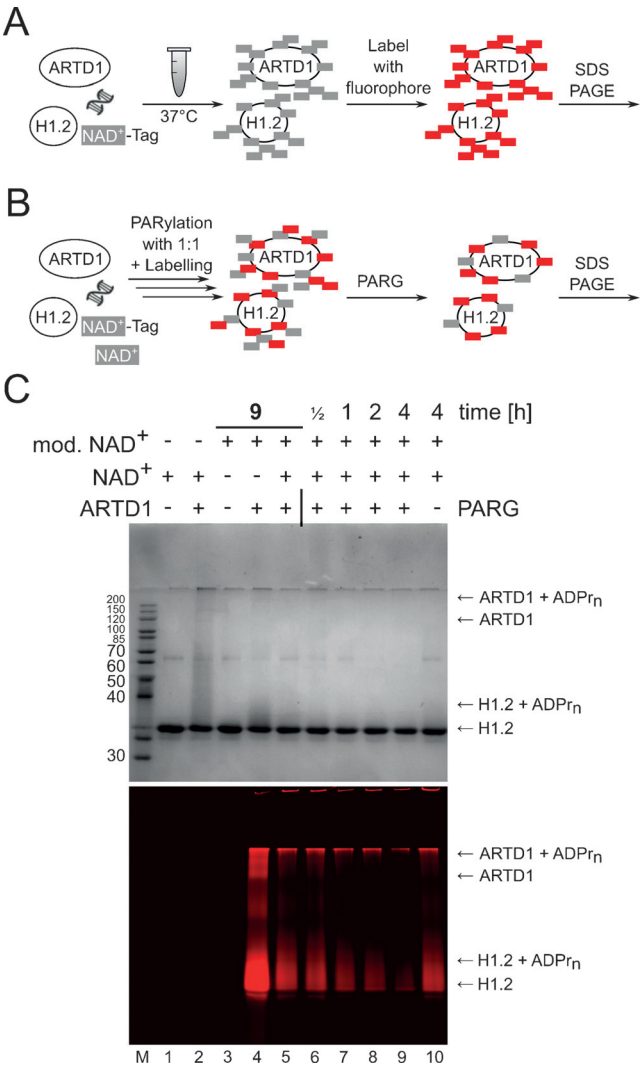


***Figure 2.*** A) Workflow of the ADP-ribosylation assay with histone H1.2. B) Workflow of the degradation test with PARG. C) Modification of H1.2 and ARTD1 with modified $NAD^+$ analogue **9** followed by SPAAC reaction, as well as a degradation test with PARG. Results were analyzed by SDS PAGE. Upper panel: Coomassie Blue staining. Lower panel: Cy3 fluorescence channel. Total concentration of NADs was 1 mM. Time-dependent degradation was tested following treatment with a 1:1 mixture of **9** and natural $NAD^+$. A sample without PARG was used as a control.

Having revealed good tolerance of 2-modified NADs by ARTD1, we next explored other reporters to eventually achieve higher labeling efficiency. To avoid the non-specific staining of cyclooctyne fluorophores, we pursued a reverse approach and coupled cycloocytne DIBAC for reaction with azide-functionalized dyes to $NAD^+$, since this is one of the fastest SPAAC reagents ($k_2 = 0.31 \pm 0.02\ m^{-1}s^{-1}$).[20] For this, adenosine **19**, which bears an amine-protected linker, was synthesized (Scheme 1).[21] After phosphorylation and deprotection, the free amine reacts with DIBAC-NHS ester to form the modified adenosine monophosphate **23**. Coupling with β-nicotinamide monophosphate gave **9**. In addition, we added

  

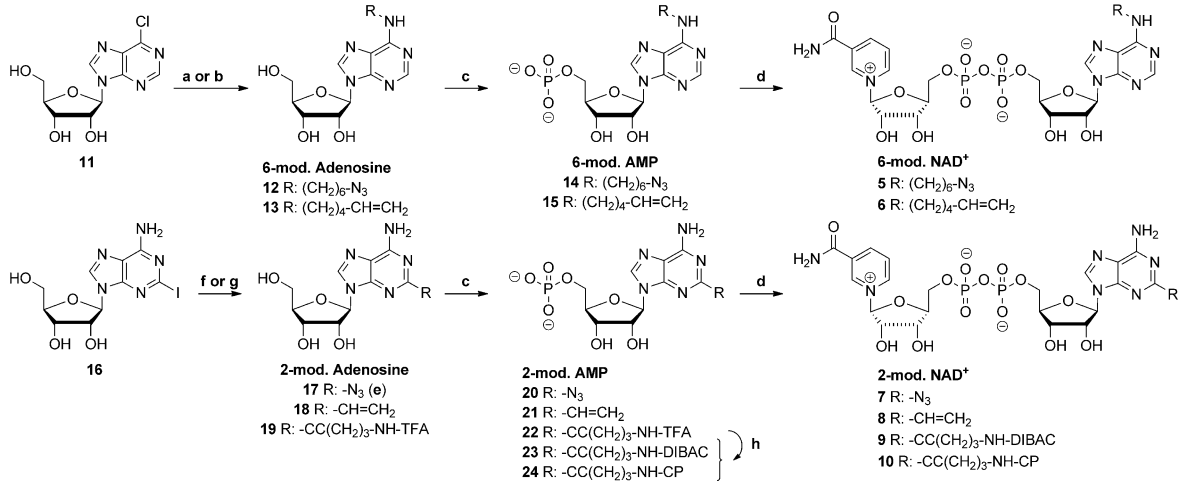


***Scheme 1.*** Syntheses of $NAD^+$ analogues **5**–**10**. Reaction conditions: a) 6-azidohexane-1-amine, EtOH, 80 °C, 3 h, 61 %; b) 5-hexen-1-amine, EtOH, 80 °C, 3 h, 49 %; c) $POCl_3$, proton sponge, TMP, 0 °C, 1–3 h, 40–60 %; d) β-NMN, CDI, $NEt_3$, DMF, RT, 96 h 20–60 %; e) prepared according to different literature method; f) trifluoro-*N*-(pent-4-yn-1-yl)acetamide, CuI, $Pd(PPh_3)_4$, DMF, RT, 16 h, 83 %; g) $Bu_3SnCH=CH_2$, $Pd(PPh_3)_4$, NMP, 100 °C, 2 d, 92 %; h) 1. 25 % $NH_4OH$, RT, 30 min, 2. DIBAC-NHS or CP nitrophenyl carbonate, 0.1 M $NaHCO_3$ pH 8.7, DMF, 16 h, 32–54 %. TMP = Trimethylphosphate, β-NMN = β-Nicotinamide monophosphate, CDI = *N*,*N*′-Carbonyldiimidazole, DMF = *N*,*N*-dimethylformamide, NMP = *N*-Methyl-2-pyrrolidone, DIBAC = 4-(11,12-didehydrodibenzo[*b*,*f*]azocin-5(6*H*)-yl)-4-oxobutanoic acid, CP = (2-methylcycloprop-2-en-1-yl)methyl, AMP = adenosine monophosphate, NHS = *N*-hydroxysuccinimide, TFA = trifluoroacetate.

a recently developed cyclopropene functionality to $NAD^+$, assuming that fast reaction kinetics ($k_2 = 0.99 \pm 0.1\ m^{-1} s^{-1}$)[17] would prevent excessive background staining by tetrazine-functionalized fluorophores. Likewise, deprotected monophosphate **22** was coupled to (2-methylcycloprop-2-en-1-yl)methyl 4-nitrophenyl carbonate to give **24**, which was reacted with β-nicotinamide monophosphate to obtain **10** (Scheme 1). Testing compounds **9** and **10** in the assay revealed that both are accepted by ARTD1 despite their bulky modifications (Figure 2C and Figure S3). Moreover, these analogues are also incorporated into PAR in the presence of natural $NAD^+$ (Figure 2C, Lane 5), thus identifying them as competitive substrates. Furthermore, we investigated whether poly(ADP-ribose) glycohydrolase[22] (PARG), the major PAR degrading enzyme, can also cleave these modified chains. H1.2 was PARylated with a 1:1 mixture of **9** and $NAD^+$ and then labeled by SPAAC. After stopping the reaction with the ART inhibitor olaparib,[23] the reaction mixture was then incubated with PARG, which led to exoglycosidic cleavage of ADP-ribose except for the first moieties (Figure 2B). As shown in Figure 2C (Lanes 6–9), the fluorescent PAR chains are degraded with increasing reaction time.

After positive evaluation of the analogues in vitro, we advanced their cellular application. Hela cells were stressed with $H_2O_2$ to induce DNA damage and stimulate PAR formation. At the same time, the $NAD^+$ analogues were introduced into the cells through transient permeabilization of the cell membrane.[24] After fixation, labeling reactions were performed with the respective dyes. As controls, cells were either not exposed to $H_2O_2$, pre-incubated with olaparib, or treated with natural $NAD^+$. By using confocal fluorescence imaging, we found that azide-functionalized dyes, which are used in SPAAC and CuAAC, result in high signal-to-noise ratios, which makes them the first choice for the in-cell visualization of PAR (see Figure 3 and S4A). Interestingly, the fluorescent signal was nearly suppressed below the detection limit when ARTD1 activity was knocked down[25] through the use of siRNA (Figure S5). This indicates that the cytochemical signals detected originate from the action of a single enzyme, namely ARTD1.

In line with recent reports,[26] incubation with cyclooctyne- and tetrazine-functionalized dyes led to unspecific staining inside cells. Hence, selective labeling with 2-azido-$NAD^+$ **7**

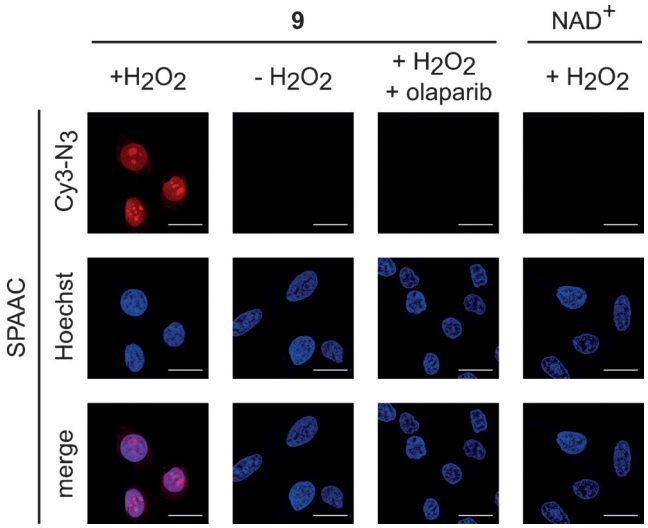


***Figure 3.*** Visualization of intracellular poly(ADP-ribose) formation using $NAD^+$ analogue **9** and SPAAC chemistry. Hela cells were treated with $H_2O_2$, transiently permeabilized, incubated with **9**, and fixed. Labeling was performed by SPAAC with Cy3-$N_3$ and DNA was stained with Hoechst 33342. Controls were performed without $H_2O_2$ treatment, with the inhibitor olaparib, and with natural $NAD^+$. Samples were analyzed by confocal microscopy. Scale bars: 20 μm.

  

through SPAAC was not achieved with cyctooctyne-functionalized dyes because the signal was indistinguishable from the background, even after iodoacetamide treatment[27] (Figure S6). Staining in the cytosol is also observed with tetrazine-functionalized fluorophores, but can be controlled by applying low dye concentrations and fast reaction kinetics as shown with analogue **10** (Figure S4B).

Next, we explored whether the analogues are suited to the simultaneous detection of PARylation in two-color labeling experiments, for example, as required in pulse–chase studies. We therefore administered a 1:1 mixture of **9** and **10** according to the described method and labeled the samples with azide- and tetrazine-functionalizeddyes in one step and with two colors. As controls, samples treated with only one analogue or with natural $NAD^+$ were processed in the same manner. When the two analogues were applied, positive staining in the nucleus was observed in both fluorescence channels, whereas each analogue alone was only labeled in its corresponding color (see Figure 4). These experiments demonstrate the potential of the new compounds for future use in dual-color labeling schemes.

In summary, we synthesized six new $NAD^+$ analogues that were modified at different sites of the adenosine. By testing them in ADP-ribosylation assays, we gained new insight into the substrate scope of ARTD1. Whereas modifications to adenine positions 7 and 8 disturb the ability of the enzyme to process these analogues, small perturbations at position6 are tolerated. Most effective are 2-modified $NAD^+$ analogues, for which even long and bulky modifications are accepted. Moreover, we achieved bioorthogonal labeling of PAR through the incorporation of functionalized $NAD^+$ analogues in vitro. For the first time, we were also able to show their application in cells, where they are metabolized upon DNA damage by ARTD1. Taken together, the results indicate these analogues to be valuable tools for further biochemical and cellular studies of PARylation processes. We also demonstrated the potential to use these $NAD^+$ analogues in parallel, since their bioorthogonal design offers the opportunity for multichannel read-outs. This development of new $NAD^+$ analogues paves the way for the design of time-dependent experiments or pulse–chase applications and should thus contribute to our understanding of the highly dynamic PAR metabolism.

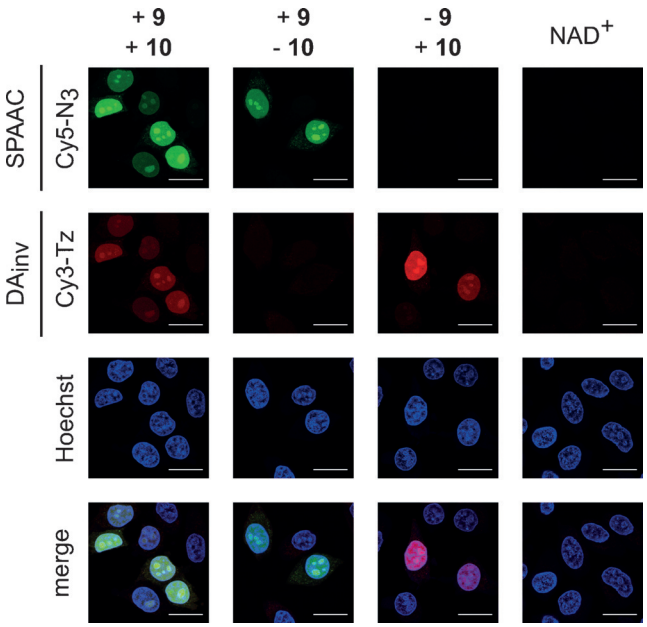


***Figure 4.*** Dual labeling of poly(ADP)ribose using **9** and **10** (1:1) with SPAAC and $DA_{inv}$. Hela cells were treated with $H_2O_2$, transiently permeabilized, incubated with the respective $NAD^+$ analogues, and fixed. Labeling was performed by simultaneous incubation with Cy5-$N_3$ and Cy3-Tz, and DNA was stained with Hoechst 33342. Controls were performed with single $NAD^+$ analogues and natural $NAD^+$. Scale bars: 20 μm.

## Acknowledgements

Financial support by Konstanz Research School Chemical Biology and DFG (SFB 969) is gratefully acknowledged. S.W. acknowledges the "Beilstein Institut zur Förderung der Chemischen Wissenschaften" and A.B. the Deutsche Telekom Stiftung for stipends. We thank B. A. Kottwitz for assistance with cell culture experiments and A. Mangerich for kindly providing siRNA.

**Keywords:** ADP-ribosylation · bioorthogonal reactions · poly(ADP-ribose) · protein modification

**How to cite:** *Angew. Chem. Int. Ed.* **2016**, *55*, 7660–7664
*Angew. Chem.* **2016**, *128*, 7790–7794

[1] a) P. Chambon, J. D. Weill, P. Mandel, *Biochem. Biophys. Res. Commun.* **1963**, *11*, 39–43; b) L. Virág, *Mol. Aspects Med.* **2013**, *34*, 1043–1045; c) W. L. Kraus, *Mol. Cell* **2015**, *58*, 902–910.
[2] B. A. Gibson, W. L. Kraus, *Nat. Rev. Mol. Cell Biol.* **2012**, *13*, 411–424.
[3] a) C. J. Pears, C. A.-M. Couto, H.-Y. Wang, C. Borer, R. Kiely, N. D. Lakin, *Cell Cycle* **2012**, *11*, 48–56; b) A. Pines, L. H. Mullenders, H. van Attikum, M. S. Luijsterburg, *Trends Biochem. Sci.* **2013**, *38*, 321–330.
[4] a) S. Messner, M. O. Hottiger, *Trends Cell Biol.* **2011**, *21*, 534–542; b) W. L. Kraus, M. O. Hottiger, *Mol. Aspects Med.* **2013**, *34*, 1109–1123; c) K. W. Ryu, D.-S. Kim, W. L. Kraus, *Chem. Rev.* **2015**, *115*, 2453–2481.
[5] a) P. Bai, *Mol. Cell* **2015**, *58*, 947–958; b) P. Bai, C. Cantó, *Cell Metab.* **2012**, *16*, 290–295.
[6] F. Aredia, A. I. Scovassi, *Front. Biosci. Elite Ed.* **2014**, *6*, 308–317.
[7] a) M. I. Rodríguez, J. Majuelos-Melguizo, J. M. M. Martín-Consuegra, M. R. de Almodóvar, A. López-Rivas, F. J. Oliver, *Med. Res. Rev.* **2015**, *35*, 678–697; b) A. Mangerich, A. Bürkle, *Int. J. Cancer* **2011**, *128*, 251–265.
[8] M. O. Hottiger, P. O. Hassa, B. Lüscher, H. Schüler, F. Koch-Nolte, *Trends Biochem. Sci.* **2010**, *35*, 208–219.
[9] Z. Tao, P. Gao, H.-w. Liu, *J. Am. Chem. Soc.* **2009**, *131*, 14258–14260.
[10] N. P. Westcott, H. C. Hang, *Curr. Opin. Chem. Biol.* **2014**, *23*, 56–62.
[11] a) H. Kawamitsu, H. Hoshino, H. Okada, M. Miwa, H. Momoi, T. Sugimura, *Biochemistry* **1984**, *23*, 3771–3777; b) J. H. Küpper, L. van Gool, M. Müller, A. Bürkle, *Histochem. J.* **1996**, *28*, 391–395.

  

[12] G. Timinszky, S. Till, P. O. Hassa, M. Hothorn, G. Kustatscher, B. Nijmeijer, J. Colombelli, M. Altmeyer, E. H. K. Stelzer, K. Scheffzek, M. O. Hottiger, A. G. Ladurner, *Nat. Struct. Mol. Biol.* **2009**, *16*, 923 – 929.
[13] a) H. Jiang, J. H. Kim, K. M. Frizzell, W. L. Kraus, H. Lin, *J. Am. Chem. Soc.* **2010**, *132*, 9363 – 9372; b) Y. Wang, D. Rösner, M. Grzywa, A. Marx, *Angew. Chem. Int. Ed.* **2014**, *53*, 8159 – 8162; *Angew. Chem.* **2014**, *126*, 8298 – 8301; c) I. Carter-O'Connell, H. Jin, R. K. Morgan, L. L. David, M. S. Cohen, *J. Am. Chem. Soc.* **2014**, *136*, 5201 – 5204.
[14] V. V. Rostovtsev, L. G. Green, V. V. Fokin, K. B. Sharpless, *Angew. Chem. Int. Ed.* **2002**, *41*, 2596 – 2599; *Angew. Chem.* **2002**, *114*, 2708 – 2711.
[15] N. J. Agard, J. A. Prescher, C. R. Bertozzi, *J. Am. Chem. Soc.* **2004**, *126*, 15046 – 15047.
[16] A.-K. Späte, V. F. Schart, S. Schöllkopf, A. Niederwieser, V. Wittmann, *Chem. Eur. J.* **2014**, *20*, 16502 – 16508.
[17] A.-K. Späte, H. Bußkamp, A. Niederwieser, V. F. Schart, A. Marx, V. Wittmann, *Bioconjugate Chem.* **2014**, *25*, 147 – 154.
[18] A. Bourderioux, P. Naus, P. Perlíková, R. Pohl, I. Pichová, I. Votruba, P. Džubák, P. Konečný, M. Hajdúch, K. M. Stray, T. Wang, A. S. Ray, J. Y. Feng, G. Birkus, T. Cihlar, M. Hocek, *J. Med. Chem.* **2011**, *54*, 5498 – 5507.
[19] a) S. Higashiya, C. Kaibara, K. Fukuoka, F. Suda, M. Ishikawa, M. Yoshida, T. Hata, *Bioorg. Med. Chem. Lett.* **1996**, *6*, 39 – 42; b) L. Wicke, J. W. Engels, *Bioconjugate Chem.* **2012**, *23*, 627 – 642; c) S. M. Hacker, F. Mortensen, M. Scheffner, A. Marx, *Angew. Chem. Int. Ed.* **2014**, *53*, 10247 – 10250; *Angew. Chem.* **2014**, *126*, 10413 – 10416.
[20] M. F. Debets, S. S. van Berkel, S. Schoffelen, F. P. J. T. Rutjes, J. C. M. van Hest, F. L. van Delft, *Chem. Commun.* **2010**, *46*, 97 – 99.
[21] S. M. Hacker, N. Hardt, A. Buntru, D. Pagliarini, M. Mockel, T. U. Mayer, M. Scheffner, C. R. Hauck, A. Marx, *Chem. Sci.* **2013**, *4*, 1588 – 1596.
[22] K. Hatakeyama, Y. Nemoto, K. Ueda, O. Hayaishi, *J. Biol. Chem.* **1986**, *261*, 14902 – 14911.
[23] K. A. Menear, C. Adcock, R. Boulter, X.-l. Cockcroft, L. Copsey, A. Cranston, K. J. Dillon, J. Drzewiecki, S. Garman, S. Gomez, H. Javaid, F. Kerrigan, C. Knights, A. Lau, V. M. Loh, I. T. W. Matthews, S. Moore, M. J. O'Connor, G. C. M. Smith, N. M. B. Martin, *J. Med. Chem.* **2008**, *51*, 6581 – 6591.
[24] a) D. Koley, A. J. Bard, *Proc. Natl. Acad. Sci. USA* **2010**, *107*, 16783 – 16787; b) A. B. Neef, N. W. Luedtke, *ChemBioChem* **2014**, *15*, 789 – 793.
[25] L. Efremova, S. Schildknecht, M. Adam, R. Pape, S. Gutbier, B. Hanf, A. Bürkle, M. Leist, *Br. J. Pharmacol.* **2015**, *172*, 4119 – 4132.
[26] H. E. Murrey, J. C. Judkins, C. W. am Ende, T. E. Ballard, Y. Fang, K. Riccardi, L. Di, E. R. Guilmette, J. W. Schwartz, J. M. Fox, D. S. Johnson, *J. Am. Chem. Soc.* **2015**, *137*, 11461 – 11475.
[27] R. van Geel, G. J. M. Pruijn, F. L. van Delft, W. C. Boelens, *Bioconjugate Chem.* **2012**, *23*, 392 – 398.

Received: January 15, 2016
Revised: February 29, 2016
Published online: April 15, 2016

  